JOURNAL OF GEOPHYSICAL RESEARCH, VOL. 106, NO. D17, PAGES 20,101–20,113, SEPTEMBER 16, 2001

South Pole submillimeter sky opacity and correlations with radiosonde observations

Richard A. Chamberlin

Caltech Submillimeter Observatory, Hilo, Hawaii, USA

Abstract. Submillimeter wave-length observations of the South Pole wintertime atmospheric opacity were performed on a regular basis starting in the year 1992. The absorption spectrum of pressure broadened water vapor lines is known to dominate submillimeter atmospheric transparency, and changes in opacity should be correlated with changes in the precipitable water vapor column (PWV). Indications of PWV were derived from radiosonde observations and the expected correlation with opacity was observed. Thus submillimeter radiometry can be used to predict radiosonde derived PWV and vice versa. These comparisons can be used to help interpret radiosonde PWVs. For example, we show that the absolute calibration of one instrument type, the A.I.R. Model 5A, in use at the South Pole since February 22, 1997, is doubtful and indicates wintertime PWVs about a factor of 2 smaller than expected when compared to opacity and PWV relationships established previously. Comparisons were also made to PWV_{sat}, the precipitable water vapor column derived by assuming saturation over ice. Radiosonde data going back to 1961 were available, and we examined long-term trends in the wintertime PWV and PWV_{sat}. The primary emphasis here was to reveal the expected long-term site quality of the South Pole for performing ground based submillimeter astronomy. Thus we focused on wintertime conditions. Our comparisons of submillimeter opacity to PWV also provide robust determinations of the magnitude of dry air opacity, important for improving submillimeter radiative transfer models.

1. Introduction

Millimeter and submillimeter opacity is well correlated with precipitable water vapor column density [*Zammit and Ade*, 1981]. Here, and previously, we extend these observations of correlation between submillimeter atmospheric opacity and water vapor column to an extremely dry and cold site: the South Pole. We find that there is significant correlation between the South Pole precipitable water vapor column (PWV) derived from routine radiosonde observations and routine submillimeter atmospheric opacity measurements [*Chamberlin and Bally*, 1995; *Chamberlin et al*., 1997]. The observed correlations allow quantitative determinations of the dry air opacity and the opacity dependence on water vapor column. This result can be used for improving radiative transfer models and is also useful for astronomical site characterization as we can use daily, routine radiosonde observations to predict sky opacity on days when submillimeter opacity was not measured [*Chamberlin and Bally*, 1995; *Chamberlin et al*., 1997]. A good site for performing ground-based submillimeter astronomy has an atmosphere with very low water vapor and very high temporal stability. The South Pole atmosphere meets these conditions [*Smythe and Jackson*, 1977; *Dragovan et al*., 1990; *Chamberlin and Bally*, 1994, 1995; *Chamberlin et al*., 1997; *Lay and Halverson*, 2000]. The scope of the present work is limited to the South Pole wintertime period since it is when the lowest water vapor conditions prevail. Portions of the present work were previously presented at the American Astronomical Society Meeting, San Diego, California, June 1998; the National Radio Science meeting, Boulder, Colorado, January 1999; the Antarctic Automatic Weather Station meeting, Byrd Polar Research Center, Columbus, Ohio, May 2000; the International Astronomical Union meeting, Marrakech, Morroco, November 2000; and published in abstract form [*Chamberlin*, 1999].

Paper number 2001JD900208.
0148-0227/01/2001JD900208$09.00

There are possible problems with most radiosonde types operating in the Antarctic environment including hysteresis, sensitivity, and calibration at cold temperature. Despite these possible problems, submillimeter radiometric opacity has a significant correlation with radiosonde derived PWV. The observed correlation provides a strong indication that standard radiosonde types used at the South Pole in very cold weather are responding to tropospheric integrated water vapor column density in a statistically repeatable way. For example, in 1992 [*Chamberlin and Bally*, 1995], on average, we observed self-consistency between PWV derived from measurements made with A.I.R. Model 4A radiosondes using VIZ (VIZ Manufacturing Co., Philadelphia, Pennsylvania) carbon hygrometers [*Potts and Savitz*, 1990], 25 NOAA ozonesonde soundings between days 249 and 335 using a Vaisala capacitive hygrometer, and concurrent submillimeter 225-GHz opacity measurements. In the present work we will provide further evidence that the A.I.R. Model 4A system was, on average, providing accurate indications of tropospheric PWV.

In case of doubt about the absolute accuracy of humidity sensor derived PWV, it is also possible to use the temperature profile in each radiosonde ascent record to set an upper limit on the measurable PWV by assuming water vapor saturation over ice [*Chamberlin and Bally*, 1995]: PWV_{sat}.

The long-term history the South Pole PWV and PWV_{sat} is useful for astronomical site characterization since it provides some indication of the year-to-year variations and an upper

Table 1. Submillimeter Opacity Data Collection History

Year	Frequency, GHz	Instrument Type
1992	225 ± 2	NRAO 225-GHz heterodyne radiometer [*Liu*, 1987; *Chamberlin and Bally*, 1994]
1995	229 ± 2	AST/RO radio telescope (heterodyne)
	490.7 ± 2	AST/RO radio telescope (heterodyne)
	493.7 ± 2	AST/RO radio telescope (heterodyne) [*Chamberlin et al*., 1997; *Stark et al*., 2001]
1997	462.5 ± 2	AST/RO radio telescope (heterodyne)
1998	229 ± 2	AST/RO radio telescope (heterodyne)
	462.5 ± 2	AST/RO radio telescope (heterodyne)
	493.7 ± 2	AST/RO radio telescope (heterodyne)
	860 ± 50	NRAO/CMU broadband radiometer—(S. Radford and J. Peterson, unpublished data)

limit on the water vapor column measurable by conventional radiosonde systems. The record of radiosonde measurements at the South Pole exists going back to before 1961. In the present work, that record shows that the South Pole site quality was consistently good every winter since 1961. (Radiosonde observations started as early as 1957, but we have not been successful in locating copies of that data.) That is, the favorable wintertime submillimeter conditions observed since 1992 are no aberration, rather they are characteristic. This finding is in contrast to what has been observed on middle-latitude, high mountain astronomical sites such as Mauna Kea whose history shows extreme interannual variability in average site quality, and thus, average PWV [*Pardo et al*., 2001, Figure 1].

Our examination of the radiosonde record since 1961 also provides some information about long-term trends in wintertime average PWV and PWV_{sat}. Any long-term trends in Antarctic tropospheric weather, including integrated water vapor column density are of interest to researchers in Antarctic meteorology [*Neff*, 1999; *Mosley-Thompson et al*., 1999]. The existence of such trends might be due to related changes in tropospheric circulation patterns induced by long-term changes in stratospheric heating related to the annual formation of the ozone hole.

Comparisons of submillimeter opacity and radiosonde derived PWV provide robust determinations of the magnitude of dry air opacity at the South Pole site [*Chamberlin and Bally*, 1995; *Chamberlin et al*., 1997]. Significant contributions to dry air opacity are caused by collision induced multipole moments in nonwater vapor gas species. Accurately modeling of dry air opacity is a topic of ongoing research [*Pardo et al*., 2001].

2. Experimental Methods

Opacity measurements were made at frequencies of astronomical interest. Narrow bandwidth submillimeter atmospheric opacity measurements were made with a National Radio Astronomy Observatory (NRAO) heterodyne site testing monitor in 1992 [*Chamberlin and Bally*, 1994; *Liu*, 1987], and with the AST/RO radio telescope in 1995 [*Chamberlin et al*., 1997], 1997, and 1998. Broad bandwidth measurements of the 860-GHz submillimeter opacity were also made in 1998 (S. Radford, NRAO, and J. Peterson, Carnegie Mellon University, unpublished data, 1998).

The submillimeter opacity was obtained by using the "skydip" method. For discussion and examples of the method, see references [*Ulich and Haas*, 1976; *Chamberlin and Bally*, 1994; *Chamberlin et al*., 1997]. Table 1 summarizes the history of overwinter opacity measurements.

Radiosonde records from 1991 and onward were obtained directly from the South Pole Meteorology office (met@spole.gov) via ftp. Records prior to 1991 were obtained from the NOAA Climate Monitoring and Diagnostics Laboratory ftp site (ftp.cmdl.noaa.gov/met/raobs/spo). Table 2 summarizes what we know about the history of radiosonde types used for routine, daily observations by the South Pole meteorological office. (Radiosonde types used in recent years were made by VIZ (VIZ Manufacturing Co., Philadelphia, Pennsylvania), and A.I.R. (Atmospheric Instrumentation Research, Boulder, Colorado). The division of VIZ that manufactured radiosondes and hygrometers was acquired by Sippican, Inc. (Marion, Massachusetts) in December 1997, and A.I.R. was acquired by Vaisala (Boulder, Colorado) in February 1999.)

Standard radiosonde types [*Gaffen*, 1992] used worldwide, including the A.I.R. Models 4A [*Atmospheric Instrumentation Research, Inc*., 1991; *Potts and Savitz*, 1990] and 5A, and the VIZ radiosondes used at the South Pole before 1991, use a transfer function to relate humidity transducer response at a given temperature to the relative humidity over liquid water, RH_w. In South Pole radiosonde reports going back to 1961, RH_w was reported directly, and that quantity was used here for deriving PWV as described previously [*Chamberlin and Bally*, 1995], and below.

Table 2. Radiosonde System History[a]

Years	Ground Station	Radiosonde	Hygrometer
1957–1961	unknown (and data not available)	unknown	unknown
1961–1976	unknown	unknown	unknown
1977–1990	Bendix GMD	VIZ	VIZ resistive
1991–1996	A.I.R.	A.I.R. Model 4A	VIZ resistive
1997–2000	A.I.R.	A.I.R. Model 5A	capacitive

[a]Sources of information: private communications from the South Pole meteorological office, 1992–2000; owing to a lack of adequate records the 1977 start date given for the Bendix GMD ground station should be considered uncertain. T. Curran (Sippican, Inc., Marion, Massachusetts) provided information about the Bendix groundstation, by private communication; the hygrometer type in the A.I.R. Model 4A is known from the Operations Manual [*Atmospheric Instrumentation Research, Inc*., 1991]; and the hygrometer type in the Model 5A was determined from bench testing by the author and also from the Model 5A data sheet provided by D. O'Conner (Vaisala, Boulder, Colorado). We note that Model 5A Operations Manual (System IS-5A1-MET, Version 1.7, 1997) is ambiguous and incorrectly implies that the Model 5A uses a VIZ hygrometer. This ambiguity probably arose from the fact that A.I.R. groundstations updated to support the Model 5A radiosondes can also support the Model 4A.

The method can be outlined as follows. Each South Pole radiosonde ascent record contains: the pressure P, height, temperature T, and the relative humidity RH_w. The reported temperature in Celsius was used in Bolton's equation to compute the saturation vapor pressure over water in mbars: $E_{w\_sat} = 6.112 \exp[(17.67T)/(T + 243.5)]$ [*Atmospheric Instrumentation Research, Inc*., 1991; *Rogers and Yau*, 1989a]. The derivation of the water vapor partial pressure E_{mb} was then straightforward: $E_{mb} = (E_{w\_sat}\, RH_w)/100$. This derivation of E_{mb} from the radiosonde data sets is the most direct method and it also exactly follows the procedure described in the Operations Manual for the A.I.R. Model 4A radiosonde [*Atmospheric Instrumentation Research, Inc*., 1991]. The derived E_{mb} were then used with the ideal gas law to determine the mass density of water vapor at each reported height. Integration of the mass density over the vertical column gave the column density of PWV in gm/cm^2. In this paper, PWV is expressed in millimeters: 1 g of water precipitated onto an area of 1 cm^2 makes a column 10 mm in height.

Since there has been some question about the absolute accuracy of the radiosonde measurements of water vapor, particularly in cold temperatures of less than −40°C *Mahesh et al*. [1997] and *World Meteorological Organization* (WMO) [1983] as quoted in the work of *Gaffen* [1992, p. 8]. We also used the reported radiosonde temperature to compute the water vapor column density with the assumption that the atmosphere was in saturation over ice, PWV_{sat}: PWV_{sat} provides an upper limit on the water vapor column detectable by conventional radiosonde systems. In the absence of supersaturation with respect to the ice phase, PWV_{sat} is the maximum water vapor the troposphere could hold. As will be described later, we believe the incidence and degree of wintertime supersaturation is not large.

The method of calculating PWV_{sat} is described previously [*Chamberlin and Bally*, 1995] and is summarized as follows:

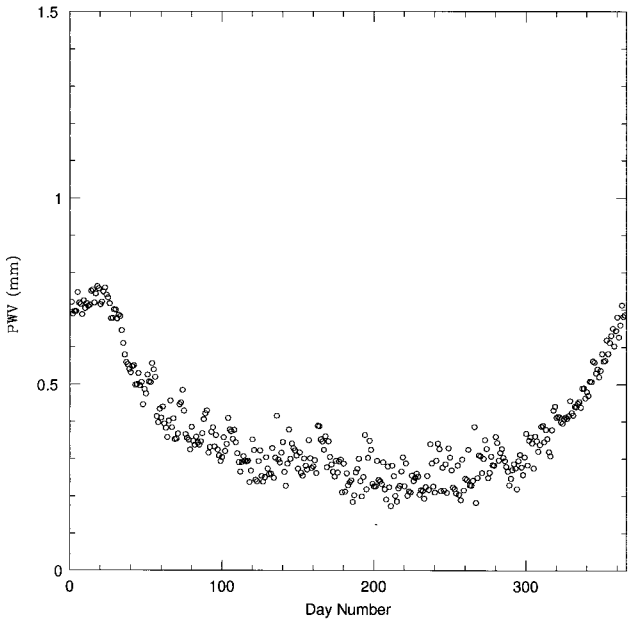

Figure 1. The average PWV derived from radiosonde observations, versus day of the year. All accepted observations (see text and Figure 3) from 1961 through 1999 were averaged together to make this plot.

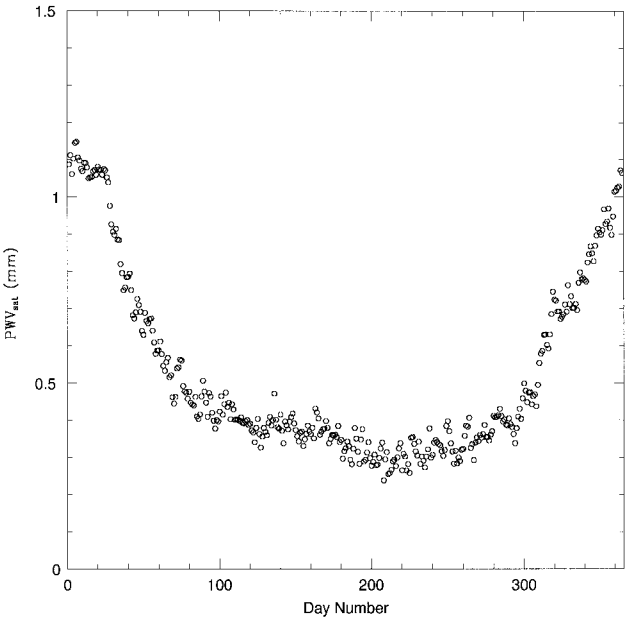

Figure 2. The average PWV_{sat} derived from radiosonde observations, versus day of the year. All accepted observations (see text and Figure 3) from 1961 through 1999 were averaged together to make this plot.

temperatures reported by the radiosonde during its ascent were used to compute the saturation vapor pressure over ice, E_{i_sat}, using an integrated form of the Clausius-Clapeyron equation [*Rogers and Yau*, 1989a]. E_{i_sat} was used with the ideal gas law to determine the mass density of water vapor and then integrated over the vertical column to give PWV_{sat}.

A limited set of NOAA radiosonde measurements using frost point hygrometers was also available (H. Vömel, University of Colorado, personal communication, 2000). The radiosonde frost point hygrometer [*Oltmans*, 1985] was developed for measuring the very low water vapor abundance in the stratosphere where conventional resistive and capacitive hygrometers have insufficient sensitivity. The device directly measures the frost point by monitoring the change in reflectivity off of a temperature controlled mirror [*Vömel et al*., 1995]. The data sets available express the water vapor abundance in ppmv as a function of altitude. The water vapor abundance in ppmv was converted into partial pressure and used with the ideal gas law to determine the mass density of water vapor which was integrated over the column to give PWV. Only a small set of data was available: 17 measurements from 1991 to 1994. Only a small set of data was available: 17 measurements from 1991 to 1994 during the period when the A.I.R. Model 4A was in use (see Table 2). Five measurements were available from 1990, but they were not used here since our interest was in comparison with the A.I.R. Model 4A response to PWV.

In this paper, the winter time comparisons were generally delimited by days 100–300, since this interval appears to be the typical period of lowest prevailing water vapor in the annual cycle, see Figures 1 and 2. Any particular 180-day subset of this period could be expected to have similar statistics. For ease of comparison with calendar days, here we defined day 1.0 to be January 1, at 0000 UT.

In all cases, the integration was cut off at the tropopause.

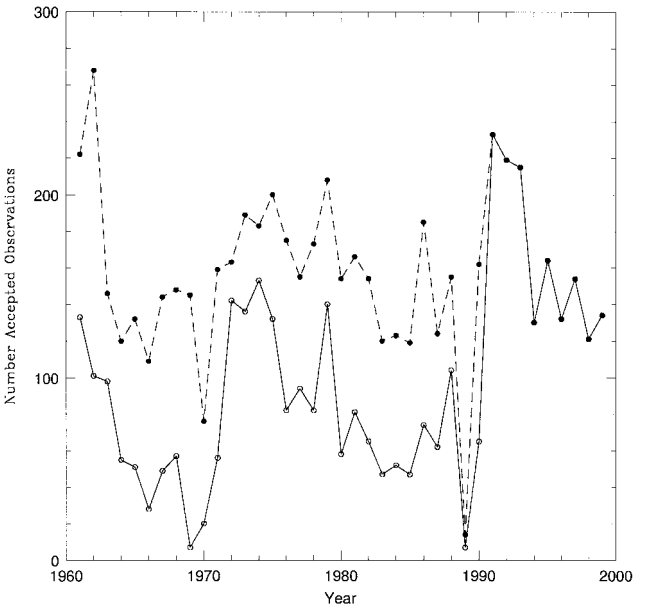

Figure 3. The dashed line indicates the number of PWV_{sat} observations, and the solid line indicates the number of PWV observations accepted each year in the winter period between days 100 and 300.

The cutoff was required because South Pole radiosonde systems using VIZ carbon hygrometers did not indicate relative humidities of less than ~20%. This floor in the sensitivity may have been deliberately imposed on the data to comply with earlier National Weather Service standards (T. Curran, Sippican, Inc., private communication, 2000). In any case the 20% floor in the sensitivity was self-evident by inspection of the radiosonde ascent records.

Prior to 1991 the height of the tropopause was assumed to be between 100 and 500 mbar, and it was defined to be the height of the first time the temperature versus altitude lapse rate became zero or negative. After 1991 we used the tropopause heights reported by the radiosonde system. The A.I.R. Model 4A and Model 5A radiosonde systems determined the tropopause by finding the lowest elevation where the lapse rate becomes less than 2°C/km and remained less than that over a 2 km change in elevation. The different tropopause acceptance criteria might contribute to a small bias in the pre-1991 tropopause determinations. However, determinations of PWV are weighted in favor of the lower troposphere where T and P are highest. Thus any small bias caused by the change has little effect on our results for PWV and PWV_{sat}.

If the balloon did not ascend to sufficient height to detect the tropopause, then the observation was rejected. If the balloon hygrometers were not working during the ascent, or if less than four values were reported during the ascent, the observation of PWV for that flight was also rejected.

Figure 3 shows the number of PWV and PWV_{sat} observations accepted each year since 1961. The dashed line connecting the solid points shows the number of PWV_{sat} observations accepted versus year, and the solid line connecting the open points shows the number of PWV observations accepted between days 100 and 300. In most winters, only one radiosonde launch per day was normal. In 1961 and 1962 two launches per day were often attempted. In 1991, 1992, and 1993, two launches per day were performed after about day number 271.

Supersaturation of some atmospheric layers with respect to ice might occasionally occur, although it seems that this effect is not significant for our purposes here, as described below and in section 3. If supersaturation did occur, it would not be directly detectable by conventional radiosonde techniques since the presence of the hygrometer detector itself initiates ice nucleation on the detector element [*Anderson*, 1994]. That is, the highest humidity detectable would be that which implies coexistence with the bulk ice phase.

In subfreezing clouds a mixed phase water/ice regime exists between $0°C \geq T \geq T_{glac}$ [*Baker*, 1997]. Below T_{glac} all water is frozen out. The magnitude of T_{glac} is highly variable: $-10° \gtrsim T_{glac} \gtrsim -35°$, depending on cloud type and history. The factors influencing the magnitude of T_{glac} and ice nucleation in subfreezing temperatures are complex and still under active research but a few general principles are well established: the concentration of ice in subfreezing clouds increases sharply with decreasing temperature; in the mixed phase regime, collision of ice and supercooled droplets often leads to accretion with rapid freezing of the super-cooled water [*Rogers and Yau*, 1989b]; in the mixed phase regime, secondary processes can greatly enhance the number density of ice nucleation centers [*Mossop*, 1985]; sedimentation from frozen layers above may seed new ice nucleation [*Hall and Pruppacher*, 1976]; the type and history of the cloud is important and older clouds of the same type generally contain more ice; and any ice already present will reduce supersaturation by absorbing vapor into diffusional growth of existing ice crystals [*Rogers and Yau*, 1989b]. In the South Pole winter period the average ground temperature is about −58°C and rises through a step inversion to about −36°C in the stratified isothermal layer which is ~500–1000 meters above the surface [*Schwerdtfeger*, 1984]. Moisture in the cold, stratified isothermal layer is advected from maritime sources far away and during its wintertime transport over the continent this moist layer is continuously

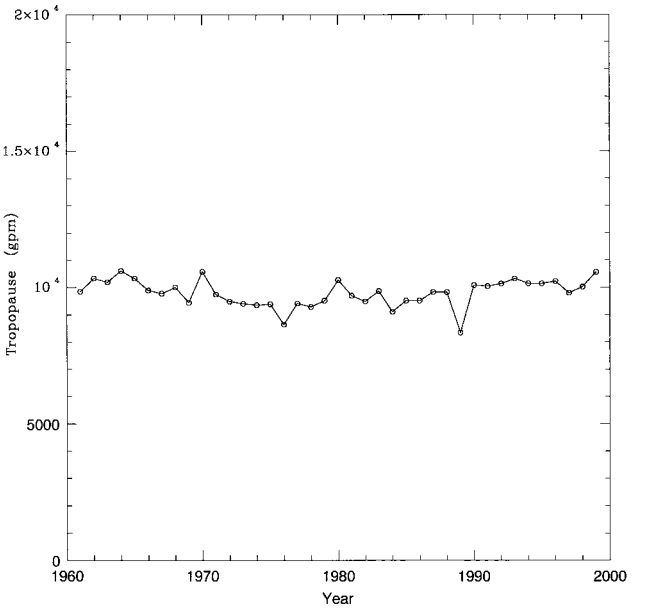

Figure 4. The average tropopause height in the winter period, versus year. The height is given in geopotential meters (gpm), but at 10,000 m the difference between geopotential meters and meters above mean sea level (msl) is only 0.2%. For our purposes here the difference is negligible.

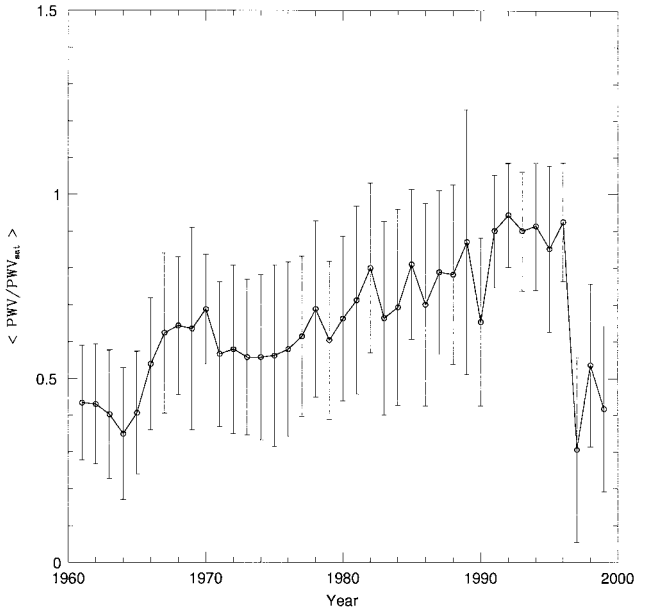

Figure 5. PWV/PWV$_{sat}$ was computed for each day that valid observations exist, and the annual average, ⟨PWV/PWV$_{sat}$⟩, is shown versus year. The error bars are the standard deviation in each average.

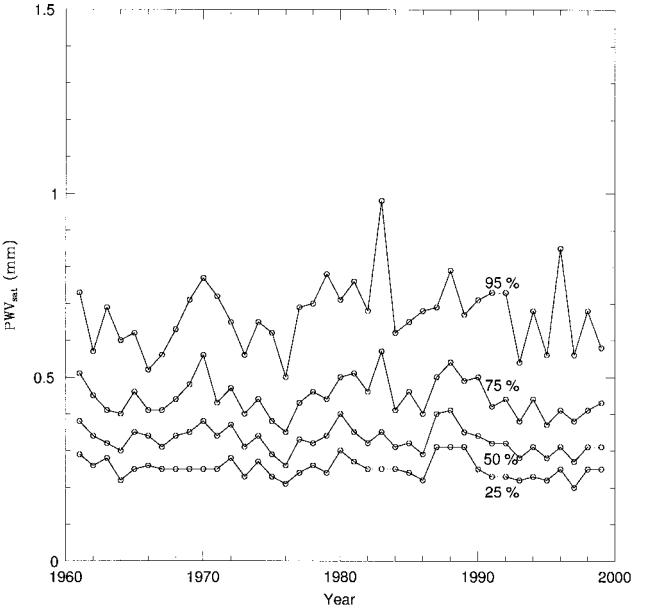

Figure 7. PWV$_{sat}$ cumulative distribution versus year for the winter period, days 100 to 300. For example, this graph shows that in 1992 the PWV$_{sat}$ was equal to or less than 0.23 mm 25% of the time, 0.32 mm 50% of the time, 0.44 mm 75% of the time, and 0.73 mm 95% of the time. The lower solid line connects points delimiting the 25% cumulative distribution level, the second solid line from the bottom connects points delimiting the 50% cumulative distribution level, etc.

cooled by radiating heat into colder layers above and below [*Schwerdtfeger*, 1984]. These circumstances imply relatively long equilibration times for moist layers that would work against the persistence of supersaturation with respect to ice. If supersaturation in any of the lower tropospheric layers did exist, the effect would be to underreport RH$_w$ in those layers, and then overreport RH$_w$ in higher and dryer layers until the ice condensed on the detector was sublimated. In that case, the effect on RH$_w$ would be hysteretic and tend to partially cancel in the calculation of PWV since it is an integrated quantity. If all layers were supersaturated (and assuming ideal instrument performance) then PWV and PWV$_{sat}$ would be identical but underreport the true water vapor abundance. However, as noted, the circumstances of the wintertime South Pole troposphere would not appear to favor the persistence of significant supersaturation with respect to ice. In section 3 we present some experimental evidence indicating ice supersaturation, if it existed, did not have significant effect on our derived values of PWV.

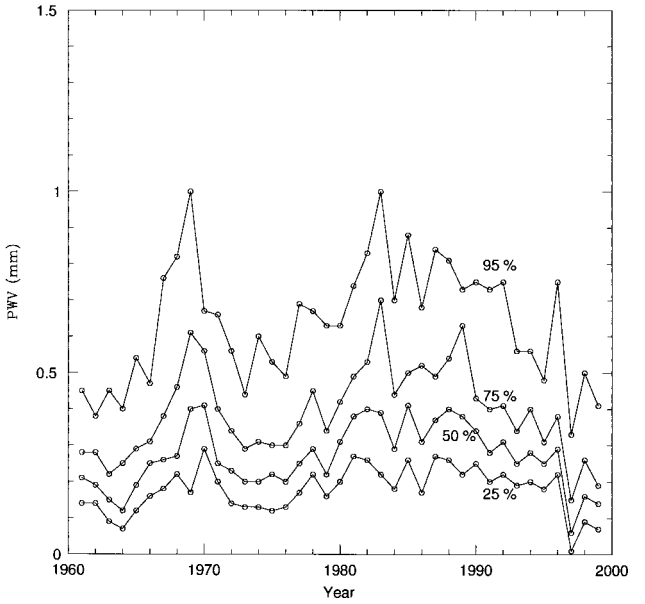

Figure 6. PWV cumulative distribution versus year for the winter period, days 100–300. For example, this graph shows that in 1992 the PWV was equal to or less than 0.22 mm 25% of the time, 0.31 mm 50% of the time, 0.41 mm 75% of the time, and 0.75 mm 95% of the time. The lower solid line connects points delimiting the 25% cumulative distribution level, the second solid line from the bottom connects points delimiting the 50% cumulative distribution level, etc.

In our derivations of PWV and PWV$_{sat}$ we have ignored water vapor in the stratosphere and above, but this contribution should not be large: ~4 ppmv [*Mahesh et al*., 1997; *Vömel et al*., 1995]. Also, we have not attempted to compensate for the instrument hysteresis apparent when the radiosondes are rising through the rapidly changing inversion layer near the surface [*Mahesh et al*., 1997]. Since this hysteretic effect can only be estimated and may be variable between instruments even of the same model type, we prefer to leave it out of the derivations of PWV and PWV$_{sat}$. Neglecting hysteresis in the inversion layer may imply that water vapor is underreported at lower altitudes and overreported at higher altitudes. Since PWV and PWV$_{sat}$ are integrated quantities, these two effects cancel to some extent. Neglecting the stratospheric water vapor and hysteresis may cause some slight systematic bias in the derived PWV and PWV$_{sat}$, but it should have little effect on the relative comparisons between different years.

Table 3. Wintertime PWV Cumulative Distribution and Average Tropopause Height[a]

Year	25%	50%	75%	95%	Days	OBS	REJ	Tropopause Height
1961	0.14	0.21	0.28	0.45	85	133	250	9848.
1962	0.14	0.19	0.28	0.38	68	101	284	10331.
1963	0.09	0.15	0.22	0.45	95	98	104	10197.
1964	0.07	0.12	0.25	0.40	53	55	150	10609.
1965	0.12	0.19	0.29	0.54	51	51	138	10330.
1966	0.16	0.25	0.31	0.47	28	28	153	9893.
1967	0.18	0.26	0.38	0.76	49	49	161	9776.
1968	0.22	0.27	0.46	0.82	54	57	149	10005.
1969	0.17	0.40	0.61	1.00	7	7	211	9444.
1970	0.29	0.41	0.56	0.67	20	20	111	10578.
1971	0.20	0.25	0.40	0.66	51	56	169	9740.
1972	0.14	0.23	0.34	0.56	130	142	75	9486.
1973	0.13	0.20	0.29	0.44	120	136	68	9404.
1974	0.13	0.20	0.31	0.60	132	153	74	9353.
1975	0.12	0.22	0.30	0.53	116	132	97	9388.
1976	0.13	0.20	0.30	0.49	73	82	151	8637.
1977	0.17	0.25	0.36	0.69	84	94	134	9410.
1978	0.22	0.29	0.45	0.67	72	82	157	9282.
1979	0.16	0.22	0.34	0.63	106	140	120	9515.
1980	0.20	0.31	0.42	0.63	52	58	170	10274.
1981	0.27	0.38	0.49	0.74	72	81	152	9692.
1982	0.26	0.40	0.53	0.83	61	65	167	9487.
1983	0.22	0.39	0.70	1.00	47	47	161	9869.
1984	0.18	0.29	0.44	0.70	51	52	165	9108.
1985	0.26	0.41	0.50	0.88	44	47	173	9514.
1986	0.17	0.31	0.52	0.68	63	74	161	9516.
1987	0.27	0.37	0.49	0.84	60	62	115	9829.
1988	0.26	0.40	0.54	0.81	101	104	100	9824.
1989	0.22	0.38	0.63	0.73	6	7	19	8339.
1990	0.25	0.34	0.43	0.75	52	65	164	10080.
1991	0.20	0.28	0.40	0.73	192	233	3	10043.
1992	0.22	0.31	0.41	0.75	188	219	5	10135.
1993	0.19	0.25	0.34	0.56	188	215	6	10318.
1994	0.20	0.28	0.40	0.56	130	130	53	10144.
1995	0.18	0.25	0.31	0.48	153	164	47	10139.
1996	0.22	0.29	0.38	0.75	131	132	66	10226.
1997	0.01	0.06	0.15	0.33	152	154	45	9799.
1998	0.09	0.16	0.26	0.50	120	121	83	10018.
1999	0.07	0.14	0.19	0.41	120	134	90	10558.
Average	0.18 ± .06	0.27 ± .09	0.39 ± .12	0.64 ± .17				9799 ± 495

[a]Cumulative distribution in millimeters and tropopause height in geopotential meters. See text and Figure 6 for an explanation of the cumulative distribution. Days is the total number of days accepted observations were made. OBS & REJ are the total number of observations accepted and rejected.

3. Discussion of Radiosonde Observations

Referring to Figure 3, we can see that in most years prior to 1991 many more flights were successful in measuring PWV_{sat} to the reported tropopause than in measuring PWV. That is, either hygrometer hardware in these earlier radiosondes was failing or the data acquisition algorithms used with these earlier systems rejected the humidity measurements for some other reason. At this time, we have little history or knowledge about these earlier instruments and thus cannot say more about them.

Figure 4 shows the average wintertime tropopause height determined using the methods described. The tropopause height is given in geopotential meters (gpm), but at 10,000 gpm the difference between gpm and meters of mean altitude above sea level is <0.2% [*Rogers and Yau*, 1989c]. No definite trend is noticeable.

On days when both PWV and PWV_{sat} could be accepted according to the criteria described above, we also computed the ratio PWV/PWV_{sat}. Figure 5 shows the average of that ratio, $\langle PWV/PWV_{sat} \rangle$, for each year since 1961. The error bars on the figure are the standard deviation of the averages. There is an increasing trend in $\langle PWV/PWV_{sat} \rangle$ versus year, until 1991 when the average ratio plateaus between ~85 and 95%. In 1997 the ratio drops to ~30% and stays low after that. The South Pole meteorological office used the A.I.R. Model 4A radiosonde from 1991 until February 22, 1997. On that date they changed to the A.I.R. Model 5A. The dramatic drop in $\langle PWV/PWV_{sat} \rangle$ in 1997 is due to this change in instrument type. More evidence supporting this assertion will be presented below.

Prior to 1991 the increasing trend in $\langle PWV/PWV_{sat} \rangle$ may correspond to an increasing trend in cloud cover [*Neff*, 1999], or an increasing trend in snow fall [*Mosley-Thompson et al.*, 1999]. However, at this time we think it may be somewhat tenuous to draw any conclusions from the data in Figure 5 alone unless other information can be uncovered regarding the reliability of radiosonde humidity measurements made prior to 1991.

A representation of the yearly cumulative distribution of PWV is shown in Figure 6. The lower line labeled 25% means that 25% of the observations reported and accepted that year were at that PWV value or less. For example, in 1991, 25% of the accepted observations indicated a PWV of 0.20 mm, or less; 50% a PWV of 0.28 mm or less; etc.

Table 4. Yearly Wintertime PWV_{sat} Cumulative Distribution[a]

Year	25%	50%	75%	95%	Days	OBS	REJ
1961	0.29	0.38	0.51	0.73	140	222	161
1962	0.26	0.34	0.45	0.57	156	268	117
1963	0.28	0.32	0.41	0.69	139	146	56
1964	0.22	0.30	0.40	0.60	113	120	85
1965	0.25	0.35	0.46	0.62	132	132	57
1966	0.26	0.34	0.41	0.52	108	109	72
1967	0.25	0.31	0.41	0.56	140	144	66
1968	0.25	0.34	0.44	0.63	145	148	58
1969	0.25	0.35	0.48	0.71	138	145	73
1970	0.25	0.38	0.56	0.77	65	76	55
1971	0.25	0.34	0.43	0.72	137	159	66
1972	0.28	0.37	0.47	0.65	151	163	54
1973	0.23	0.31	0.40	0.56	171	189	15
1974	0.27	0.34	0.44	0.65	156	183	44
1975	0.23	0.29	0.38	0.62	182	200	29
1976	0.21	0.26	0.35	0.50	152	175	58
1977	0.24	0.33	0.43	0.69	134	155	73
1978	0.26	0.32	0.46	0.70	143	173	66
1979	0.24	0.34	0.44	0.78	156	208	52
1980	0.30	0.40	0.50	0.71	140	154	74
1981	0.27	0.35	0.51	0.76	151	166	67
1982	0.25	0.32	0.46	0.68	134	154	78
1983	0.25	0.35	0.57	0.98	120	120	88
1984	0.25	0.31	0.41	0.62	117	123	94
1985	0.24	0.32	0.46	0.65	114	119	101
1986	0.22	0.29	0.40	0.68	158	185	50
1987	0.31	0.40	0.50	0.69	122	124	53
1988	0.31	0.41	0.54	0.79	149	155	49
1989	0.31	0.35	0.49	0.67	13	14	12
1990	0.25	0.34	0.50	0.71	122	162	67
1991	0.23	0.32	0.42	0.73	192	233	3
1992	0.23	0.32	0.44	0.73	188	219	5
1993	0.22	0.28	0.38	0.54	188	215	6
1994	0.23	0.31	0.44	0.68	130	130	53
1995	0.22	0.28	0.37	0.56	153	164	47
1996	0.25	0.31	0.41	0.85	131	132	66
1997	0.20	0.27	0.38	0.56	152	154	45
1998	0.25	0.31	0.41	0.68	120	121	83
1999	0.25	0.31	0.43	0.58	120	134	90
1995	0.22	0.28	0.37	0.56	153	164	47
1996	0.25	0.31	0.41	0.85	131	132	66
1997	0.20	0.27	0.38	0.56	152	154	45
1998	0.25	0.31	0.41	0.68	120	121	83
1999	0.25	0.31	0.43	0.58	120	134	90
Average	0.25 ± .03	0.33 ± .04	0.44 ± .05	0.67 ± .09			

[a]Cumulative distribution is in millimeters. See text and Figure 6 for an explanation of the cumulative distribution. Days is the total number of days accepted observations were made. OBS is the total number of observations accepted. REJ is the number of observations rejected.

A representation of the yearly cumulative distribution of PWV_{sat} is shown in Figure 7. The year to year variation, particularly at the 25, 50, and 75% levels is not nearly as pronounced as in the case of PWV versus year (Figure 6). Tables 3, 4, and 5 numerically summarize all of the radiosonde results discussed in this section.

The absolute response of the A.I.R. Model 4A to tropospheric integrated water vapor column density is validated by comparing it to the limited set of data available from radiosonde flights using the NOAA frost point hygrometer (see Figure 8). The daily A.I.R. Model 4A flights were not exactly concurrent with launch times of the National Oceanic and Atmospheric Administration (NOAA) radiosondes, so adjacent measurements bracketing the NOAA radiosonde launch times were interpolated. Only 16 of the 17 NOAA flights are shown as one of the launches could not be bracketed owing to a missed A.I.R Model 4A launch. As demonstrated in Figure 8, the agreement was generally quite good. The line drawn through the scatterplot is a best fit line with a slope of 1.0 and an intercept of 0.04.

Since the temperature of the frost point mirror is actively controlled, it should be possible for it to servo to temperatures above ambient and directly detect the extent of ice supersaturation should it exist, unlike conventional radiosonde hygrometers [*Anderson*, 1994]. Thus the good agreement observed in Figure 8 is also an indication that supersaturation with respect to the ice phase is not generally a significant effect in the South Pole wintertime lower troposphere, at least with respect to its effect on our derivations of PWV.

4. Correlations of Submillimeter Opacity and PWV

Submillimeter atmospheric opacity is strongly influenced by water vapor absorption. In this section we will show that data acquired at frequencies across the submillimeter spectrum in

Table 5. Yearly Wintertime Average of the Daily PWV/PWV_{sat}[a]

Year	$\langle PWV/PWV_{sat} \rangle$	$\pm\sigma$	OBS
1961	0.434	0.156	133
1962	0.430	0.163	101
1963	0.402	0.175	98
1964	0.349	0.180	55
1965	0.406	0.167	51
1966	0.539	0.179	28
1967	0.624	0.218	49
1968	0.643	0.187	57
1969	0.635	0.274	7
1970	0.688	0.149	20
1971	0.566	0.197	56
1972	0.579	0.228	142
1973	0.558	0.211	136
1974	0.558	0.225	153
1975	0.562	0.247	132
1976	0.579	0.237	82
1977	0.614	0.218	94
1978	0.688	0.239	82
1979	0.604	0.215	140
1980	0.662	0.224	58
1981	0.712	0.255	81
1982	0.800	0.230	65
1983	0.664	0.262	47
1984	0.693	0.266	52
1985	0.809	0.203	47
1986	0.700	0.275	74
1987	0.788	0.221	62
1988	0.782	0.244	104
1989	0.871	0.360	7
1990	0.653	0.228	65
1991	0.901	0.152	233
1992	0.943	0.142	219
1993	0.901	0.162	215
1994	0.913	0.173	130
1995	0.852	0.226	164
1996	0.925	0.161	132
1997	0.306	0.252	154
1998	0.536	0.222	121
1999	0.417	0.226	134

[a]Here σ is the standard deviation in each yearly average. OBS is the number of observations accepted to form each yearly average.

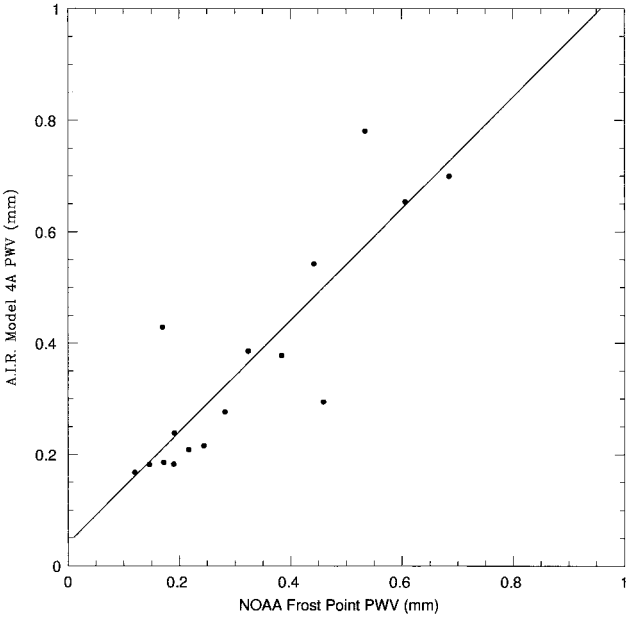

Figure 8. PWV from the A.I.R Model 4A compared to 16 radiosonde flights using the NOAA frost point hygrometer.

1998 can be correlated with the PWV measurements derived from radiosonde flights of the A.I.R. Model 5A system in use at the South Pole since February 22, 1997. Previously, we showed that (1) in 1992, 225-GHz opacity data were well correlated with PWV derived from the A.I.R. Model 4A radiosondes and NOAA ozonesondes [*Chamberlin and Bally*, 1995] and (2) in 1995, 492-GHz opacity data were also well correlated with the PWV from the A.I.R. Model 4A system [*Chamberlin et al*., 1997]. In comparing the pre and post 1997 correlations we will show that the newer Model 5A's now in use are indicating PWV's with a factor of ~2 less than expected based on earlier measurements of submillimeter opacity and PWV. This finding would also be in agreement with the change in the ratio $\langle PWV/PWV_{sat} \rangle$ in Figure 5, if PWV_{sat} was relatively constant from year to year, which is in fact what is indicated in Figure 7. For example, the average of all years at the 25% cumulative distribution level gives PWV = 0.18 ± 0.06, and PWV_{sat} = 0.25 ± 0.03 (see Tables 3 and 4). The relative yearly variation of PWV at this cumulative distribution level was ~30%, whereas the yearly variation of PWV_{sat} was ~12%. Similar relative differences are observed at the other cumulative distribution levels: i.e., with all years averaged, the interannual variation of PWV was ~30%, and the interannual variation of PWV_{sat} was ~12% at all cumulative distribution levels. If only years 1991 through 1996 are averaged (years when only the A.I.R. Model 4A was used), then at the 25% level, PWV = 0.20 ± .02, a variation of 10% which is similar to PWV_{sat} for all years.

Figure 9 shows a time series of the submillimeter opacity and PWV data in 1998. Figure 9a is the broad bandwidth NRAO/CMU 860-GHz (τ860) opacity time series (S. Radford and J. Peterson, unpublished data, 1998); Figures 9b, 9c, and 9d are the narrow bandwidth 493.7-GHz (τ493.7), 462.5-GHz (τ462.5), and 229-GHz (τ229) opacity time series; and Figure 9e is the PWV time series derived from observations made with the A.I.R. Model 5A radiosonde system. The broad bandwidth opacity measurements centered on 860 GHz covers about ±50 GHz, and the other narrow bandwidth measurements (±2 GHz) at lower frequencies are previously unpublished data acquired with heterodyne receivers on the AST/RO submillimeter radiotelescope [*Stark et al*., 2001].

Figure 10 compares concurrently measured submillimeter opacity and PWV. In Figures 10a, 10c, and 10d the opacity data were acquired within ±12 hours of the radiosonde launch time. Figure 10b used 860-GHz opacity data from the continuously running NRAO/CMU radiometer, and these data were accepted if they were acquired within 60 min of the radiosonde launch time. Each open circle is an individual data point. The solid lines are the result of linear regression fits: $\tau = A + B \times$ PWV. A and τ are expressed in nepers/airmass, and B is expressed in nepers/(airmass × mm_{H_2O}). In this context, the neper unit is used to describe power extinction. For example, the power transmitted through the atmosphere from a celestial source is $power_{transmitted} = power_{incident} \times \exp(-\tau \times$ airmass). The argument of the exponent, $\tau \times$ airmass, is in nepers [*Kraus*, 1986] and Airmass ≅ 1/cos (ZA) where ZA is zenith angle of the celestial source with respect to the observer on the earth's surface.

In Figures 10a and 10d, the triangular points were excluded

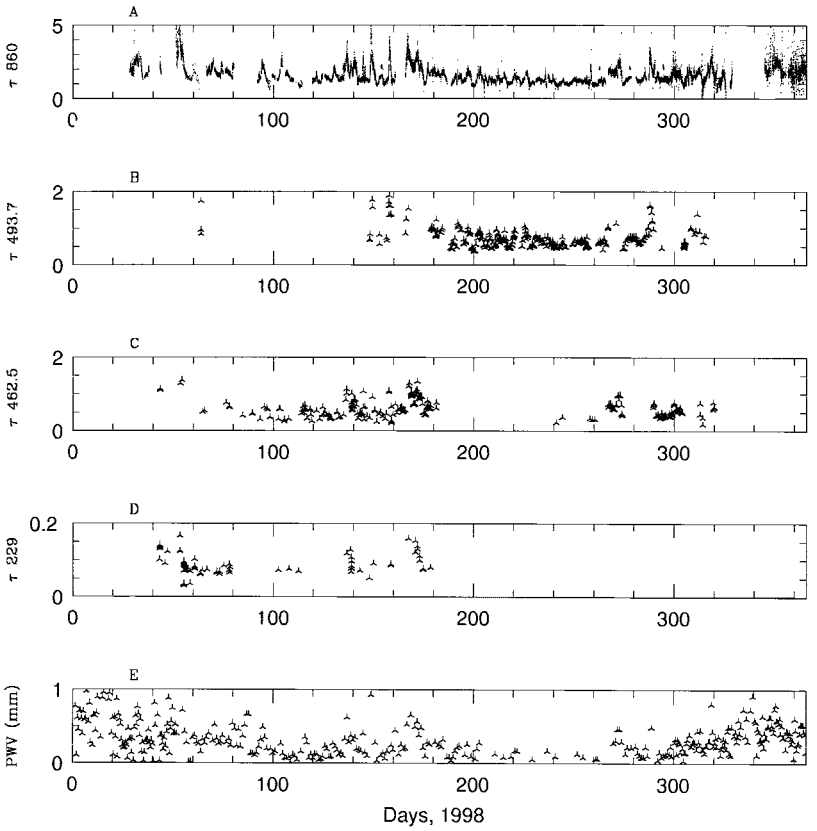

Figure 9. (a) The 860-GHz opacity versus day number in 1998; (b, c, d) 493.7-, 462.5-, and 229-GHz opacities; and (e) radiosonde derived PWV.

from the fit. These points appear to be due to anomalous radiosonde data collected on day 43. Elimination of these points in Figure 10a has little effect on the intercept and slope since there are many other data, but it has more effect on the data in Figure 10d since there are relatively fewer points.

Table 6 summarizes the results of the linear regression fits for 1998 and all other years as well. In each case, A is the intercept, or so called "dry air opacity"; B is the slope, $\Delta\tau/\Delta$PWV; R is the linear correlation coefficient; and N is the number of points used for the fit.

As expected, these scatterplots indicate a significant relationship between the opacity and PWV. For example, at 493.7 GHz, R is 0.77 for 87 points compared. If τ and PWV were completely uncorrelated, then obtaining R as large as 0.77 would be extremely unlikely. Similar statements can be made about the linear fits of τ to PWV at other frequencies. In all cases the correlations are significant.

Comparisons for other years were made previously, and Table 6 also summarizes these results. We can see that in some years previous and subsequent to 1997, opacity at the same frequencies were measured. For example, in 1995 and in 1998, opacities at 229 and 493.7 GHz where measured.

As we have seen, in years after 1996 when the radiosonde type was switched, there was a problem with the reported PWV's. This problem should show up in the B coefficients of Table 6. The problem does show up: comparisons of B values obtained at the same frequencies in 1995 and 1998 indicate that PWV's derived from A.I.R. Model 5A are a factor of 1.7 less than those derived from Model 4A measurements.

Another estimate of the change in PWV response with change in instrument type can be obtained from $\langle \mathrm{PWV}/\mathrm{PWV}_{\mathrm{sat}} \rangle$. The 1991 to 1996 radiosonde data indicate the interannual variation of $\langle \mathrm{PWV}/\mathrm{PWV}_{\mathrm{sat}} \rangle$ is relatively small: $\langle \mathrm{PWV}/\mathrm{PWV}_{\mathrm{sat}} \rangle = 0.91 \pm 0.03$. After 1996, $\langle \mathrm{PWV}/\mathrm{PWV}_{\mathrm{sat}} \rangle = 0.42 \pm 0.12$. If we assume that $\langle \mathrm{PWV}/\mathrm{PWV}_{\mathrm{sat}} \rangle$ really should be about the same from year to year, then the change in the two ratios indicates that the A.I.R. Model 5A radiosonde system was yielding wintertime PWV's a factor of 2.16 less than PWV's derived from the Model 4A system.

The indicated 2.16 correction factor was applied in Table 7 to the post 1996 PWV data and then the A and B coefficients were refit. After this correction all the B coefficients obtained at the same frequencies gave better agreement, as expected.

5. Dry Air Opacity

In section 4 we found the dry air opacity, A, by comparing τ and PWV. We observe that the South Pole wintertime PWV was so low that the submillimeter sky opacity was often dominated by dry air.

Comparisons of Tables 6 and 7 show that the dry air opacity, A, is a consistent value despite evident problems with the A.I.R. Model 5A system. This consistency shows our method of determining the dry air opacity is robust and is not too sensitive to absolute radiosonde system calibration.

Earlier, comparisons of submillimeter opacity and PWV [*Chamberlin and Bally*, 1995; *Chamberlin et al*., 1997] showed an unexpected degree of dry air opacity when compared to predictions from the Grossman AT atmospheric model for submillimeter sky transparency [*Grossman*, 1989]. At the South Pole the

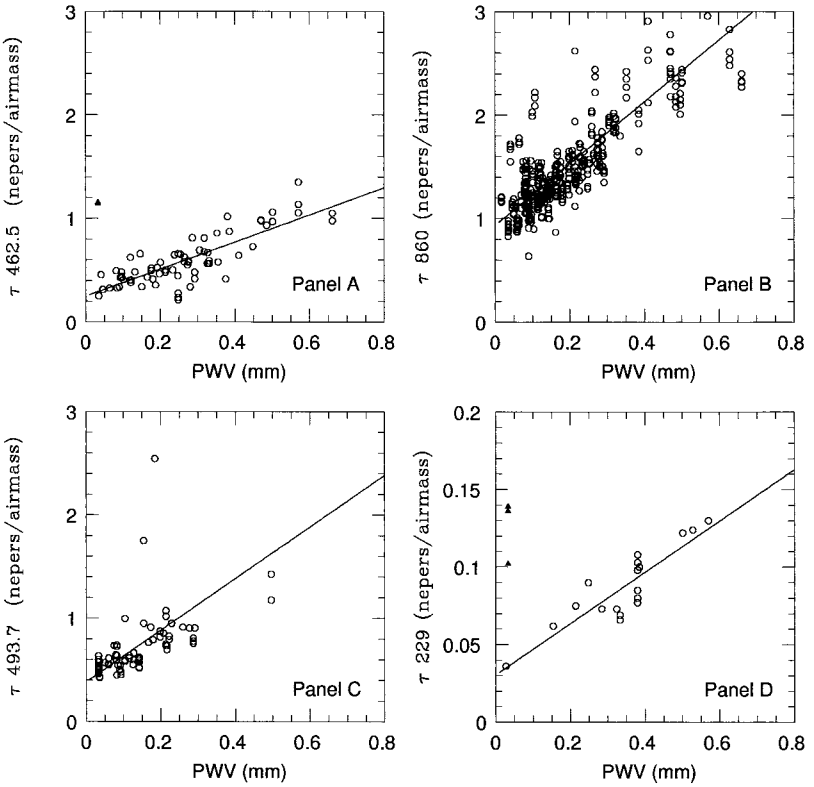

Figure 10. (a) The 462.5-GHz opacity versus PWV in 1998; (b, c, d) 860-, 493.7-, and 229-GHz opacities versus PWV. The lines through the scatterplots are the results of a linear regression best fits. The triangular points in Figures 10a and 10d are from a single radiosonde PWV measurement on day number 43. They appear to be anomalous and were excluded from the fits.

AT model generally underpredicts A by about an order of magnitude. Liebe's MPM model [*Liebe*, 1989] and Pardo et al.'s ATM model include terms for continuum emission from O_2 and N_2 and predicts a larger A but still less than what has been observed [*Chamberlin and Bally*, 1995; *Pardo et al.*, 2001].

6. Evidence for Small Inter-Annual Variations

To derive the Model 5A wintertime PWV correction factor of 2.16, we assumed that the actual, true interannual variability in $\langle PWV/PWV_{sat} \rangle$ was small from 1991 to 1999. Figure 7 shows the variability of PWV_{sat} was low, but what about PWV? Here we will use opacity statistics acquired from different years to show that the actual distribution and magnitudes of τ and PWV for 1995, 1997, and 1998 must have been quite similar. Recall, the change from the A.I.R. Model 4A to the Model 5A occurred in February 1997.

Figure 11 compares 493.7-GHz cumulative distribution of opacity values in 1995 and 1998. The cumulative distribution function is the integrated area under the normalized frequency distribution curve. In this context "frequency" indicates the number of times a certain opacity value was observed. Figure 11 shows four lines. The two solid lines are from 1995. One solid line shows the cumulative distribution for the measured daily opacity at 493.7 GHz. The opacity was measured on most, but not all days in 1995, so a systematic bias was possible which could happen, for example, if the instrument operator decided

Table 6. Opacity Versus PWV Correlations[a]

Year	Frequency, GHz	A	B	R	N
1992	225 ± 2	0.028	0.068	0.76	1075
1995	229 ± 2	0.035	0.10	0.78	39
	490.7 ± 2	0.57	1.44	0.82	63
	493.7 ± 2	0.33	1.49	0.78	160
1997	462.5 ± 2	0.37	1.39	0.80	165
1998	229 ± 2	0.030	0.166	0.88	18
	462.5 ± 2	0.25	1.31	0.82	72
	493.7 ± 2	0.34	2.50	0.77	87
	860 ± 50	0.93	3.0	0.83	402

[a]Plots of concurrent τ versus PWV were fit to $\tau = A + B \times$ PWV. Below are the experimentally determined coefficients A and B. R is the linear correlation coefficient, and N is the number points used for the fit. In this table, 1997 and 1998 data are uncorrected for the estimated error in PWV.

Table 7. Opacity Versus PWV Correlations With Corrections Applied to 1997 and 1998 Data[a]

Year	Frequency, GHz	*A*	*B*	*R*
1992	225 ± 2	0.028	0.068	0.76
1995	229 ± 2	0.035	0.10	0.78
	490.7 ± 2	0.57	1.44	0.82
	493.7 ± 2	0.33	1.49	0.78
1997	462.5 ± 2	0.37	0.63	0.80
1998	229 ± 2	0.030	0.076	0.88
	462.5 ± 2	0.25	0.60	0.82
	493.7 ± 2	0.38	1.15	0.77
	860 ± 50	0.93	1.38	0.83

[a]Here 1992 and 1995 data are unaltered. In the 1997 and 1998, data sets the *A* and *B* coefficients in Table 6 were redetermined after applying a 2.16 correction factor to PWVs derived from the A.I.R. Model 5A radiosonde system. With this correction applied to the post 1996 PWVs, we observe that the *B* coefficients for a given opacity frequency are in better agreement for different years. The *A* coefficients, indicating the dry air opacity, were not changed, or changed only slightly.

to measure τ only on "good" days. Since from Table 6 we have a known relationship between τ and PWV, we used the PWV observed on the missing days to fill in the missing τ [*Chamberlin et al*., 1997]. The second solid line shows the 1995 data including the estimation of τ for the missing days. Both lines are nearly coincident and are labeled "1995 (Raw & UA data)." Since the solid lines nearly coincide, we can say that the 1995 data set was not biased by selective observing.

The 1998 data set for the 493.7-GHz opacity was treated the same way. All four resulting plots are shown overlaid. As demonstrated by this plot, the cumulative statistics between 1995 and 1998 are virtually the same for both years, at least to the 75% cumulative distribution level. In the distributions shown on these figures, τ values from between days 100 to 322 were used. As a practical matter, good submillimeter observing can be extended well into the spring so we used this set of 223 days for these comparisons. Sometimes workers try to compare telescope sites on the basis of 90- or 180-day periods. Any subset of 180 contiguous days in this 223-day period would have a similar distribution.

Figure 12 shows the same treatment as in Figure 11 for the 1997 and 1998 462.5-GHz opacity data. These results show that 1997 and 1998 were almost statistically identical years as well. Figures 11 and 12 taken together imply that the water vapor distributions at the cumulative distribution level of 75% or smaller were similar in the years 1995, 1997, and 1998.

7. Are There Any Long-Term Trends in Wintertime Water PWV?

Figures 5 and 6 would seem to indicate that the South Pole wintertime tropospheric PWV was rising over most of the period from 1961 to 1991. However, the record is complicated by the change in instrument types over the history of the observing program and the fact that many winter periods prior to 1991 were only sparsely sampled for PWV (see Figure 3). Also unknown is the relative response of the earlier radiosonde instrument systems; whereas since 1992 we can use submillimeter opacity as a secondary standard for monitoring real, actual changes in water vapor column density.

In contrast, the PWV_{sat} cumulative distributions appear to be consistent with each other for most years (see Figure 7), and PWV_{sat} was more completely sampled (see also Figure 3). The derivation of PWV_{sat} depended only the radiosonde temperature ascent profiles. As noted, the PWV_{sat} indications were a useful indication of the maximum PWV observable by radiosonde observations, and they did not indicate an obvious trend.

We have seen that from our comparisons with other systems that the A.I.R. Model 4A was probably giving reliable indications of PWV. Between 1991 and 1996 when the A.I.R. Model

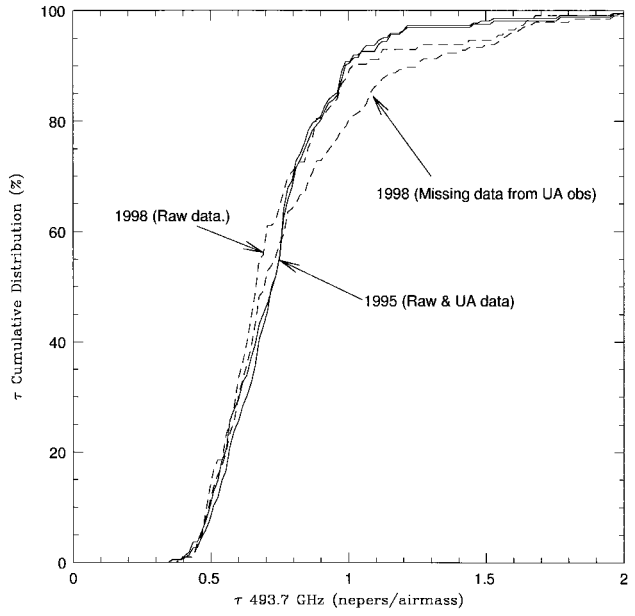

Figure 11. The cumulative distribution of 493.7-GHz daily opacity values for the years 1995 and 1998, between days 100 and days 322. This graph shows that in 1995 50% of the observed days had τ less than 0.72, 75% of the observed days had τ less than 0.83, etc. See the text for more explanation.

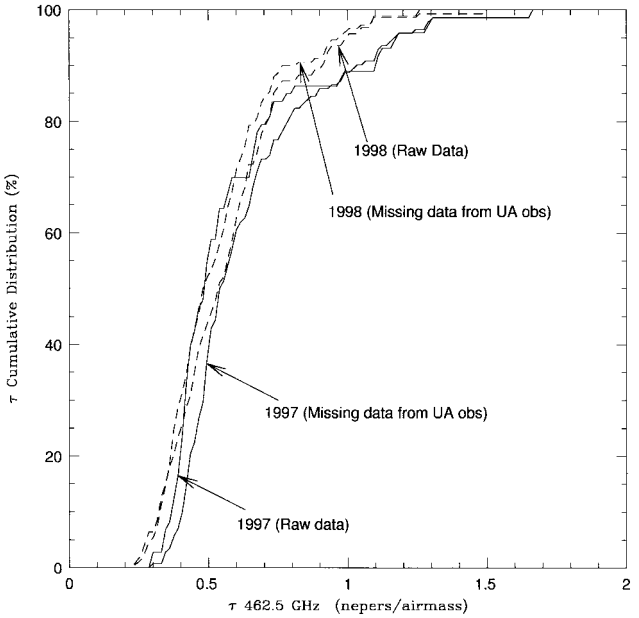

Figure 12. The cumulative distribution of 462.5-GHz daily opacity values for the years 1997 and 1998, between days 100 and days 322. See the text for more explanation.

4A system was used, and wintertime days were well sampled, there was no obvious trend apparent in PWV and during this period $\langle PWV/PWV_{sat}\rangle \approx 90\%$. That is, the magnitude of PWV was near to saturation as would seem physically reasonable in a wintertime, moist, stratified lower troposphere being continuously cooled by radiating heat into colder layers above or below [*Schwerdtfeger*, 1984].

In view of some uncertainty about pre 1991 annual PWV indications we might consider extrapolating the post 1991 result that $\langle PWV/PWV_{sat}\rangle \approx 90\%$. This general condition may well be an unavoidable consequence of the continuous radiative cooling experienced by lower tropospheric layers every winter. Also, given the fact that PWV_{sat} was generally well sampled and that its derivation relied only on simple temperature verses altitude measurements, we might conclude that for pre 1991 data, PWV_{sat} was a better indicator of water vapor trends than pre 1991 PWV.

8. Conclusions

Measurements of submillimeter opacities (τ) were always well correlated with the integrated water vapor column densities (PWV) derived from the A.I.R. Model 5A radiosonde instrument system. This correspondence is expected, and it indicates that the hygrometer detectors in the A.I.R. Model 5A instruments were responding to water vapor. However, we determined that the magnitude of the PWVs derived from the A.I.R. Model 5A instruments were low by about a factor of 2 based on comparisons of τ and PWV established previously. In addition, our comparisons of τ and PWV in the current study provided additional information about the magnitude of the dry air opacity across the submillimeter frequency band. The wintertime South Pole atmosphere is so dry that it is often dominated by the dry air opacity contribution. Measurements of dry air opacity are needed for verifying and improving radiative transfer models of the atmosphere.

In general, our investigations reflect on the validity of radiosonde derived measurements of PWV in the South Pole wintertime environment. As described earlier [*Chamberlin and Bally*, 1995], our method of correlating submillimeter opacity with radiosonde derived PWV was helpful in showing that a limited number of NOAA Ozonesonde flights in 1992 using Vaisala capacitive hygrometers generally gave the same result for PWV as the A.I.R. Model 4A using VIZ hygrometers.

In the present work, additional validation of the absolute calibration of the A.I.R. Model 4A for determining PWV was provided by comparing its results to results from a limited number of NOAA radiosonde flights using a frost point hygrometer. Good agreement was found.

In order to learn something about possible long-term trends in PWV, and also to place an upper limit on average yearly wintertime PWV which could be measured by radiosonde, we generated the quantity PWV_{sat}. PWV_{sat} is derived from only the temperature versus elevation profiles in the radiosonde ascent records, and it represents the maximum precipitable water the atmosphere could hold if it was in saturation coexisting with ice. PWV_{sat} does not rely on radiosonde hygrometer data.

As noted, the ratio $\langle PWV/PWV_{sat}\rangle$ had an increasing trend from 1961 until 1991 when the A.I.R. Model 4A came into use. While the A.I.R. Model 4A was in use from 1991 through 1996, the ratio $\langle PWV/PWV_{sat}\rangle$ was relatively stable at ~85–95%. In 1997, when the A.I.R. Model 5A came into use, $\langle PWV/PWV_{sat}\rangle$ dropped to ~30% of its previous observed value and remained consistently low through 1999, the last year covered by this study. We concluded that this sudden drop in $\langle PWV/PWV_{sat}\rangle$ was anomalous and was associated with the change in radiosonde type to the newer A.I.R. Model 5A system.

Although an increasing trend in the wintertime annual $\langle PWV/PWV_{sat}\rangle$ was indicated in the years prior to 1991, it is possible that the apparent trend may be spurious owing to uncertain radiosonde performance and calibration prior to 1991 or owing to incomplete sampling of the winter months in most years prior to 1991. In contrast, wintertime PWV_{sat}, the computation of which does not rely on hygrometer measurements, did not indicate an apparent long-term trend toward increasing values.

Acknowledgments. We thank the following individuals and groups: the staff of the South Pole meteorology office for their support in supplying data and information; Simon Radford of the National Radio Astronomy Observatory and Jeff Peterson of the Carnegie-Mellon University for sharing their broad-band 860-GHz opacity data; Tony Stark and the staff of the Antarctic Submillimeter Telescope and Remote Observatory for supplying narrowband submillimeter opacity data; Bob de Zafra, Steve Warren, and Von Walden for freely sharing information about South Pole water vapor and radiosonde; and Holger Vömel for allowing us to use NOAA frost point hygrometer data. This work was supported under the National Science Foundation grant to the Caltech Submillimeter Observatory: AST 99-80846. Travel related to this work was supported by the Center for Astrophysical Research in Antarctica and the National Science Foundation under the Cooperative Agreement OPP89-20223.

References

Anderson, P. S., A method for rescaling humidity sensors at temperatures well below freezing, *J. Atmos. Oceanic Technol*., *11*, 1388–1391, 1994.

Atmospheric Instrumentation Research, Inc., *Operations Manual, System IS-4A1-MET, Version 2.03*, p. 50, A.I.R., Inc., Boulder, Colo., 1991.

Baker, M. B., Cloud microphysics and climate, *Science*, *276*, 1072–1078, 1997.

Chamberlin, R. A., South Pole submillimeter site characteristics from heterodyne measurements (abstract), in *National Radio Science Meeting Abstracts*, p. 201, USNC/URSI Natl. Acad. of Sci., Washington, D. C., 1999.

Chamberlin, R. A., and J. Bally, 225-GHz atmospheric opacity of the South Pole sky derived from continual radiometric measurements of the sky-brightness temperature, *Appl. Opt*., *33*(6), 1095–1099, 1994.

Chamberlin, R. A., and J. Bally, The observed relationship between the South Pole 225-GHz atmospheric opacity and the water vapor column density, *Int. J. Infrared Millimeter Waves*, *16*(5), 907–920, 1995.

Chamberlin, R. A., A. P. Lane, and A. A. Stark, The 492GHz atmospheric opacity at the geographic South Pole, *Astrophys. J*., *476*, 428–433, 1997.

Dragovan, M., A. A. Stark, R. Pernic, and M. A. Pomerantz, Millimetric sky opacity measurements from the South Pole, *Appl. Opt*., *29*(4), 463–466, 1990.

Gaffen, D. J., Observed annual and interannual variations in tropospheric water vapor, *Tech. Mem. ERL ARL-198*, Natl. Oceanic and Atmos. Admin., Boulder, Colo., 1992.

Grossman, E., *AT Program*, Version 1.5, Air Head Software, Boulder, Colo., 1989.

Hall, W., and H. Pruppacher, The survival of ice particles falling from cirrus clouds in subsaturated air, *J. Atmos. Sci*., *33*, 1995, 1976.

Kraus, J. D., *Radio Astronomy*, 2nd ed., pp. 3–32, Cygnus-Quasar, Powell, Ohio, 1986.

Lay, O. P., and N. W. Halverson, The impact of atmospheric fluctuations on degree-scale imaging of the cosmic microwave background, *Astrophys. J*., *543*, 787, 2000.

Liebe, H. J., M P M—An atmospheric millimeter-wave propagation model, *Int. J. Infrared Millimeter Waves*, *10*(6), 631–650, 1989.

Liu, Z.-Y., *225GHz Atmospheric Receiver—User's Manual*, *Int. Rep. 271*, Electron. Div., Natl. Radio Astron. Obs., Charlottesville, Va., 1987.

Mahesh, A., V. P. Walden, and S. G. Warren, Radiosonde temperature measurements in strong inversions: Correlation for thermal lag based on an experiment at the South Pole, *J. Atmos. Oceanic Technol.*, *14*(1), 45–53, 1997.

Mosley-Thompson, E., J. F. Paskievitch, A. J. Gow, and L. G. Thompson, Late 20th Century increase in South Pole snow accumulation, *J. Geophys. Res.*, *104*(D4), 3877–3886, 1999.

Mossop, S. C., The origin and concentration of ice crystals in clouds, *66*(3), 264–273, 1985.

Neff, W. D., Decadel time scale trends and variability in the tropospheric circulation over the South Pole, *J. Geophys. Res.*, *104*(D22), 217–251, 1999.

Oltmans, S., Measurements of water vapor in the stratosphere with a frost-point hygrometer, *International Symposium on Moisture and Humidity*, pp. 251–258, Instrum. Soc. of Am., Research Triangle Park, N. C., 1985.

Pardo, J. R., E. Serabyn, and J. Cernicharo, Submillimeter atmospheric transmission measurements on Mauna Kea during extremely dry El Niño conditions: Implications for broadband opacity contributions, *J. Quant. Spectr. Radiat. Transfer*, *68*, 419–433, 2001.

Potts, L., and L. Savitz, Humidity sensor equations, *Tech. Pub. 80415(C)*, VIZ Manufact. Co., Philadelphia, Pa., 1990.

Rogers, R. R., and M. K. Yau, *A Short Course in Cloud Physics*, 3rd ed., pp. 12–27, Pergamon, Tarrytown, N. Y., 1989a.

Rogers, R. R., and M. K. Yau, *A Short Course in Cloud Physics*, 3rd ed., pp. 150–169, Pergamon, Tarrytown, N. Y., 1989b.

Rogers, R. R., and M. K. Yau, *A Short Course in Cloud Physics*, 3rd ed., p. 277, Pergamon, Tarrytown, N. Y., 1989c.

Schwerdtfeger, W., *Weather and Climate of the Antarctic*, pp. 28–37, Elsevier, New York, 1984.

Smythe, W. D., and B. V. Jackson, Atmospheric water vapor at the South Pole, *Appl. Opt.*, *16*(8), 2041–2042, 1977.

Stark, A. A., et al., The Antarctic Submillimeter Telescope and Remote Observatory (AST/RO), *Proc. Astron. Soc. Pac.*, *113*, 567–585, 2001.

Ulich, B. L., and R. W. Haas, Absolute calibration of millimeter-wavelength spectral lines, *Astrophys. J. Suppl.*, *30*, 247–258, 1976.

Vömel, H., S. J. Oltmans, D. J. Hofmann, T. Deshler, and J. M. Rosen, The evolution of the dehydration in the Antarctic stratospheric vortex, *J. Geophys. Res.*, *100*, 13,919–13,926, 1995.

World Meteorological Organization, Guide to meteorological instruments and methods of observations, *WMO Rep. No. 8*, Geneva, Switzerland, 1983.

Zammit, C. C., and P. A. R. Ade, Zenith atmospheric attenuation measurements at millimeter and sub-millimeter wavelengths, *Nature*, *293*, 550, 1981.

R. A. Chamberlin, Caltech Submillimeter Observatory, 111 Nowelo Street, Hilo, HI 96720, USA. (cham@ulu.submm.caltech.edu)

(Received August 24, 2000; revised February 28, 2001;
accepted March 21, 2001.)